Ground State Bleaching at Donor–Acceptor Interfaces

*Christian Schwarz, Felix Milan, Tobias Hahn, Markus Reichenberger, Stephan Kümmel, and Anna Köhler**

Charge separation at the donor–acceptor interface is a key step for high efficiency in organic solar cells. If interfacial hybrid states exist already in the dark it is plausible that they can have a major impact on the dissociation of optically generated excitations. In this work we probe such interfacial states via steady state absorption spectroscopy. A substantial bleaching of the absorption spectrum is found near the absorption edge when an electron-accepting layer of either trinitrofluorenone (TNF), C_{60}, or a perylene-diimide derivative is deposited on top of a layer of electron-donating conjugated polymers, such as MEH-PPV or various poly-phenylene. This is in part attributed to the formation of ground state complexes with low oscillator strength. The experiments bear out a correlation between the reduction of the absorbance with the energy gap between the donor-HOMO and acceptor-LUMO, the effective conjugation length of the donor, and the efficiency of exciton dissociation in the solar cell. The effect originates from mixing of the donor-HOMO and the acceptor LUMO. Calculations using density functional theory support this reasoning. Implications for efficiency of organic solar cells will be discussed.

1. Introduction

The efficiency of promising low cost organic bulk heterojunction donor–acceptor (D–A) solar cells is successively increasing over the past decade reaching now power conversion efficiencies greater than 10%.[1] These efforts are mainly based on progresses in morphology control and in the development of low bandgap materials to harvest a larger part of the sun's solar spectrum. In these solar cells ideally composited blend films with large D–A interfaces and interpenetrating networks are responsible for efficient charge separation and charge transport. A deeper understanding of the electronic processes at these donor–acceptor interfaces is needed to develop further improved strategies towards organic solar cells with even enhanced efficiencies.

For organic solar cells, the key role of photoinduced charge-transfer states in the process of dissociating an excited state at the donor–acceptor interface is well known and well documented.[2] Similarly, the intermediate formation of excited state complexes (exciplexes) in the course of electron-hole recombination has long been recognized as a central step in the operation of organic light-emitting diodes.[3]

More recently it was noted that interfacial donor–acceptor complexes with some charge-transfer character may also prevail in the ground state,[4] and that their presence and nature may impact on the photogeneration of charges.[5] Evidence for such ground state (GS) complexes is frequently brought forward by detecting the weak absorption associated with the GS complexes, for example through photothermal deflection spectroscopy.[6] A limiting case of a "donor–acceptor system" is obtained when the electron affinity of the acceptor is so strong that the acceptor may even be employed to obtain p-type doping.[7] An example for this is the acceptor molecule F4-TCNQ (2,3,5,6-tetrafluoro-7,7,8,8-tetracyanoquinodimethane). Using ultraviolet photoemission spectroscopy in combination with quantum chemical calculations, Méndez, Salzmann and co-workers have recently shown that for the D–A system comprising pentacene as donor and F4-TCNQ as acceptor, electronic interaction leads to the formation of a ground state charge-transfer complex.[8] Their work explicitly spells out and demonstrates that the frontier orbitals of the GS complex result from mixing of the highest molecular orbital (HOMO) of the donor with the lowest unoccupied molecular orbital (LUMO) of the acceptor. Both electrons in the HOMO of the GS complex then result from the former donor molecule. Salzmann and co-workers were also able to detect the weak absorption due to the GS complex.

When a GS complex is formed due to electronic interaction between a donor and an acceptor, it is not surprising that there should be an associated weak new absorption feature, with the low oscillator strength of the GS complex resulting from its charge transfer character. Concomitantly, one may expect that the original absorption from the donor polymer and the

Dr. C. Schwarz, T. Hahn, M. Reichenberger, Prof. A. Köhler
Experimental Physics II
University of Bayreuth
95440, Bayreuth, Germany
E-mail: anna.koehler@uni-bayreuth.de
Dr. C. Schwarz, T. Hahn, M. Reichenberger, Prof. A. Köhler
Bayreuth Institute of Macromolecular Research (BIMF)
University of Bayreuth
95440, Bayreuth, Germany
F. Milan, Prof. S. Kümmel
Theoretical Physics IV
University of Bayreuth
95440, Bayreuth, Germany

DOI: 10.1002/adfm.201400297

acceptor molecule that now comprise the complex should have vanished. Assessing the existence of such a ground state bleach in a quantitative manner is difficult for intermixed donor–acceptor blends. Here, we have used a bilayer geometry to compare the absorption of the donor–acceptor bilayer with the sum of the two individual layers. We observe a strong ground state bleach that we attribute to the formation of ground-state charge-transfer complexes. This lack of absorption is more intense for better conjugated chromophores. It correlates with the energy gap between the donor HOMO and the acceptor LUMO as well as with the dissociation efficiency of photo excitations. The systems investigated comprise the poly(*p*-phenylene vinylene)-type polymers MEH-PPV and PPV, the series of poly(*p*-phenylene)-type polymers MeLPPP (a ladder-type poly(*p*-phenylene)), PIF (poly-(indenofluorene)), DOOPPP (Dioctyloxy-poly(*p*-phenylene)), the solar cell "work horse" polymer P3HT (regio-regular poly(3-hexylthiophene)), and the low-bandgap polymer PCPDTBT (Poly[2,6-(4,4-bis-(2-ethylhexyl)-4*H*-cyclopenta[2,1-*b*;3,4-*b*']dithiophene)-*alt*-4,7(2,1,3-benzothiadiazole)). These donor materials were combined with the acceptor molecules TNF (2,4,7-trinitro-9-fluorenone), C_{60} and a PDI derivative (*N,N'*-bis-(1-ethylpropyl)-perylene-3,4:9,10-tetracarboxi-diimide). Given the ease of measuring the absorption of bilayers, we suggest this may provide a convenient means for initial material screening with a view to their suitability for solar cell applications.

2. Results

2.1. The Observation of a Ground State Bleach in MEH-PPV/TNF

In order to assess whether there might be any interaction between a donor and an acceptor molecule in the ground state, we compare the absorption of a bilayer film consisting of an acceptor layer on top of a donor film with the algebraic sum of the absorption of a film of donor and a film of acceptor. For this experiment, we cover a quadratic fused silica substrate

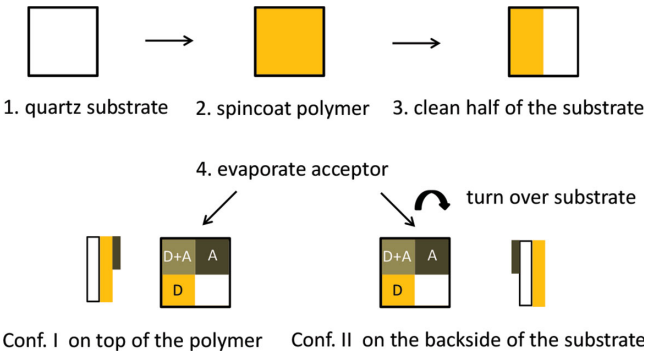

Figure 1. Scheme of the D–A interaction experiment: In configuration I the acceptor is evaporated on top of the polymer donor, in configuration II on the backside of the fused silica substrate.

with a 40 nm layer of donor polymer by spin-coating from solution. We then clean half of the substrate from the polymer layer using a cotton bud with solvent. This results in a strip of donor film. Orthogonal to the donor strip, we then evaporate a strip of an acceptor layer of 50 nm thickness using a shadow mask. As illustrated in **Figure 1**, this results in four areas of the sample prepared by the same fabrication process, that is the donor layer on its own, the acceptor layer on its own, a bilayer with acceptor on top of the donor and an uncoated area for reference. We refer to this arrangement where donor and acceptor are in contact at the bilayer as configuration I. For comparison, we also employ a configuration II, where we turn over the fused silica substrate prior to the acceptor evaporation, so that the donor and acceptor are physically separated by the quartz substrate, while still obtaining the three areas of donor, acceptor, and their superposition. If there was no interaction between donor and acceptor, one might expect that both configurations should yield the same absorption spectra. As is demonstrated in **Figure 2** for the donor–acceptor pair of MEH-PPV and TNF, the absorption spectra of MEH-PPV and of TNF are identical in both configurations. For the area where donor and acceptor overlap, there is, however, a striking difference. In configuration II, where donor and acceptor are separated by

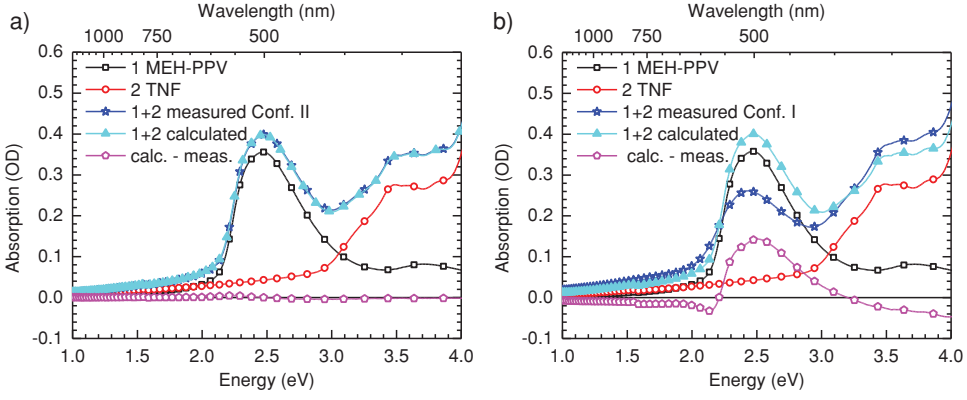

Figure 2. Absorption spectra of the different film areas in the samples prepared a) in configuration II and b) in configuration I. The black line with squares and the red line with circles show the absorption spectra measured for the areas containing only a film of MEH-PPV or TNF, respectively. The dark blue line with stars shows the absorption measured for the area where MEH-PPV and TNF films overlap. The algebraic sum of the MEH-PPV film spectrum and the TNF film spectrum is shown as light blue line with triangles. The difference between the calculated and measured superposition spectra is shown as pink line with pentagons.

the fused silica substrate, the resulting measured absorption (dark blue line with star symbols) perfectly matches the algebraic sum of the absorption spectra of the individual donor and acceptor layers (light blue line with triangle symbols). When subtracting the measured spectrum from the sum of the individual spectra, a flat line of zero intensity results (pink line with pentagons). In contrast in configuration I, where the acceptor is directly deposited onto the donor, the spectrum obtained by measuring the bilayer (dark blue line with star symbols) differs from the sum of the donor and acceptor spectra (light blue line with triangle symbols). This difference is displayed by the pink line with pentagons. Compared to the direct superposition of the individual spectra, the bilayer shows a lack of absorption in the spectral range characteristic for the $S_1 \leftarrow S_0$ absorption of MEH-PPV, centered around 2.5 eV. At this energy, the bilayer in configuration I absorbs only about 65% of the light compared to the superposition in configuration II. Furthermore, the peak of the bilayer absorption is shifted to the red by about 30 meV compared to the peak of the superposition spectrum. While the intensity of the first absorption band in MEH-PPV is reduced in the bilayer, we find an additional absorption signal below the absorption edge of MEH-PPV, that is, below 2.2 eV, as well as in the ultraviolet spectral range (3.2–4.0) eV.

2.2. The Role of the Acceptor Molecule

The observation of an altered bilayer absorption spectrum is not limited to the MEH-PPV/TNF system but also occurs for other acceptors such as C_{60} and a perylene-diimide derivative (PDI). **Figure 3** shows the absorption spectra obtained for the combination of the insoluble polymer poly(*p*-phenylene vinylene) (PPV) with C_{60}. To prepare the sample, a soluble precursor-polymer is deposited from solution and converted into

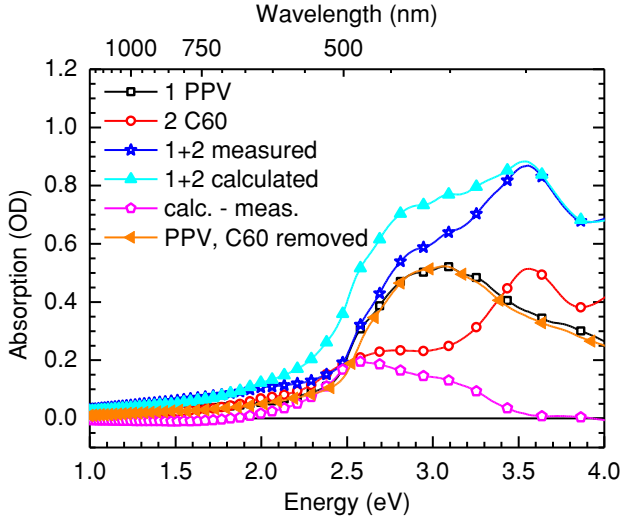

Figure 3. Absorption spectra of the different film areas in the samples prepared in configuration I, for the combination of a 41 nm film of PPV with about 30 nm of C_{60}. Lines and symbols are used analogously to Figure 2. In addition, the orange line with tilted triangles shows the absorption of the former bilayer area after the C_{60} had been mechanically removed.

an insoluble layer of PPV by heating. In this way, we prepared a sample consisting of 41 nm of PPV with about 30 nm of C_{60} on top of it in the geometry of configuration I, that is, two stripes orthogonal to each other, with direct contact between donor and acceptor in the bilayer formed by the stripes' overlapping area. Analogous to the case of MEH-PPV with TNF, we find that the absorption of the bilayer (dark blue line with triangles) differs from the sum of the absorption of the individual layers (light blue line with stars). The absorption that is missing matches the absorption of PPV from about 2.5 eV to 3.5 eV, and it also follows the absorption of the C_{60} in the range from about 1.8 eV to 2.8 eV. At the peak of the polymer absorption band, at 3.1 eV, the absorption in the bilayer is reduced by 28% compared to the sum of the individual layers. Above 3.5 eV, absorption is not missing, and centered around 1.6 eV, there seems to be a very small additional absorption signal. The reduction of the $S_1 \leftarrow S_0$ absorption band in PPV is analogous to that in MEH-PPV, while the reduction in acceptor absorption is a new feature. Before considering the reduction in acceptor absorption in more detail, we draw the reader's attention to an extension of this absorption experiment. Compared to MEH-PPV, PPV is characterized by a high packing density of the polymer backbone due to the lack of side chains, a high glass transition temperature, and concomitantly a hard surface.[9] We can therefore remove the evaporated layer of C_{60} simply by swiping over the film with a dry cotton bud. If we then measure the sample again (orange line with tilted triangles), we find a spectrum that is identical to that of the individual PPV layer measured previously. From the fact that the PPV absorption is recovered by wiping with a dry cotton bud we infer that C_{60} does not significantly diffuse into the PPV layer within the timeframe of the experiment. This implies that the lack of absorption originates from a reversible donor–acceptor interaction at the bilayer interface.

We now attend to the issue of reduced acceptor absorption indicated in the measurement of the PPV/C_{60} bilayer. The contributions of donor and acceptor absorption can be identified more clearly when compounds are used that display well-structured absorption spectra. In **Figure 4**a, we therefore consider the pair of MeLPPP as donor with a PDI derivative as acceptor. The absorption spectra of the individual compounds show well-resolved peaks. As for the previous samples, the absorption of the bilayer (dark blue line with stars) is reduced compared to the sum of the individual layers (light blue line with triangles). The difference spectrum (pink line with circles) can be matched by combining the spectra of the individual layers in the form $I_{\text{Difference}} = 0.17 I_{\text{MeLPPP}} + 0.34 I_{\text{PDI}}$. In other words, 17% of the polymer absorption are lacking as well as 34% of the PDI derivative absorption. This experiment shows that not only the polymer $S_1 \leftarrow S_0$ absorption is reduced but also the acceptor $S_1 \leftarrow S_0$ absorption. To probe whether this is indeed due to an electronic interaction between donor and acceptor, we conducted a control experiment where the MeLPPP was replaced by a 40 nm layer of the electronically inert polymer polystyrene. When polystyrene is used, the bilayer absorption spectrum is nearly identical to the spectrum obtained by the addition of the two individual layers (Figure 4b).

With the aim to probe whether the observed bilayer absorption spectrum and its intensity is free from measurement

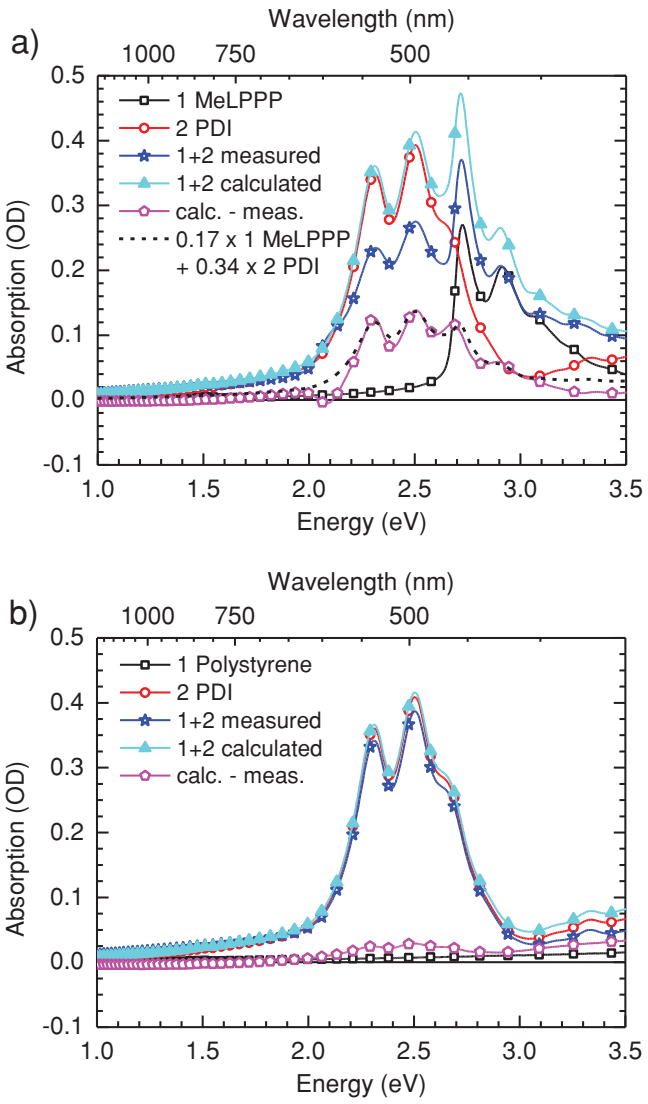

Figure 4. a) Absorption spectra of a of the different film areas in the samples prepared in configuration I for MeLPPP and a PDI derivative, with lines and symbols used analogous to Figure 2. In addition, the dashed line shows the calculated linear combination of the spectra measured for the MeLPPP-only and PDI derivative-only areas. b) The same for polystyrene and the PDI derivative.

artefacts, we performed a number of auxiliary experiments. The associated spectra are displayed in the Supporting Information. i) For a MeLPPP and PDI derivative system, we measured the absorption spectra with and without an integrating sphere. We found no significant changes between the two, suggesting that the influence of light scattering and reflection is negligible. ii) The spectra obtained are independent on the direction of the light path, that is, whether the light is incident first onto the donor layer or first onto the acceptor layer makes no difference, thus excluding optical and scattering effects. This is most evident for the MeLPPP/PDI derivative bilayer which has a well-resolved spectrum. iii) We wondered whether the changes to the polymer absorption may be related to annealing effects caused by thermal radiation of the evaporation source when the acceptor is evaporated. To test this hypothesis for the polymers MEH-PPV, MeLPPP, and PPV, we heated the evaporation source without acceptor material in it yet at the same source temperature and for the same length of time used as for an acceptor evaporation while having the polymer film in its usual place. We found the polymer absorption to be unaltered by this process. We take these auxiliary experiments to confirm that the difference between the observed bilayer absorption and the superposition of the individual spectra is a genuine signature of the material system.

2.3. The Relation of the Missing Absorption to Solar Cell Performance

From the above mentioned experiments it appears that absorption is missing in the bilayer as a result of some interaction at the interface between a π-conjugated donor polymer and a π-conjugated acceptor molecule. We were wondering whether this bleaching of the ground state absorption correlates in some way with the performance of the donor–acceptor system in solar cells. We had previously considered exciton dissociation in a series of poly(*p*-phenylene)-(PPP)-based polymers in combination with TNF or C_{60} as acceptors in a bilayer solar cell.[10] When measuring the photocurrent as a function of the internal field in the device, we found the photocurrent to increase with the applied field until it saturates for a critical field strength F_{sat}, roughly at about 100% internal quantum yield. The value of the saturation field, where exciton dissociation into charges is at its maximum, reduces with increasing effective conjugation length of the PPP-type polymer. We shall now compare this to the bleaching of the ground state absorption that we find in the associated donor–acceptor bilayers. The polymers considered are MeLPPP, which is a ladder-type PPP with a stiff backbone, a polyindenofluorene (PIF) where three phenyl rings are bridged to form a stiff unit, and a PPP with sidechains (DOOPPP) where each phenyl ring can rotate. The chemical structures are given elsewhere.[10] As acceptor we use TNF since it has less overlap with the donor absorption spectra than C_{60}, which is beneficial for the analysis. For all three donor–acceptor combinations, the measured absorption in the bilayer is lower than the mathematical superposition of the individual donor and acceptor absorption (**Figure 5**). Absorption is bleached in particular in the lower energy range of the polymer absorption band, such that the bleach signal appears like a red-shifted absorption spectrum of the polymer, even matching the vibrational structure. The amount of the polymer ground state bleach, compared to the superposition of the individual donor and acceptor signal, is summarized in **Table 1** for the PPP-type polymers and MEH-PPV in combination with TNF. Also listed are the saturation field F_{sat} required for maximum exciton dissociation, the HOMO level of the polymer and the energy difference ΔE_{gap} between the polymer HOMO and the acceptor LUMO. For MEH-PPV and MeLPPP, about 35% of the absorption is missing. In contrast, for PIF and DOOPPP, the absorption is reduced by only 27 and 11%, respectively. This amount of ground state bleaching correlates with the energy gap between donor HOMO and acceptor LUMO which is lower for MEH-PPV and MeLPPP than for PIF and DOOPPP. Importantly, it also parallels the critical field strength F_{sat} needed for

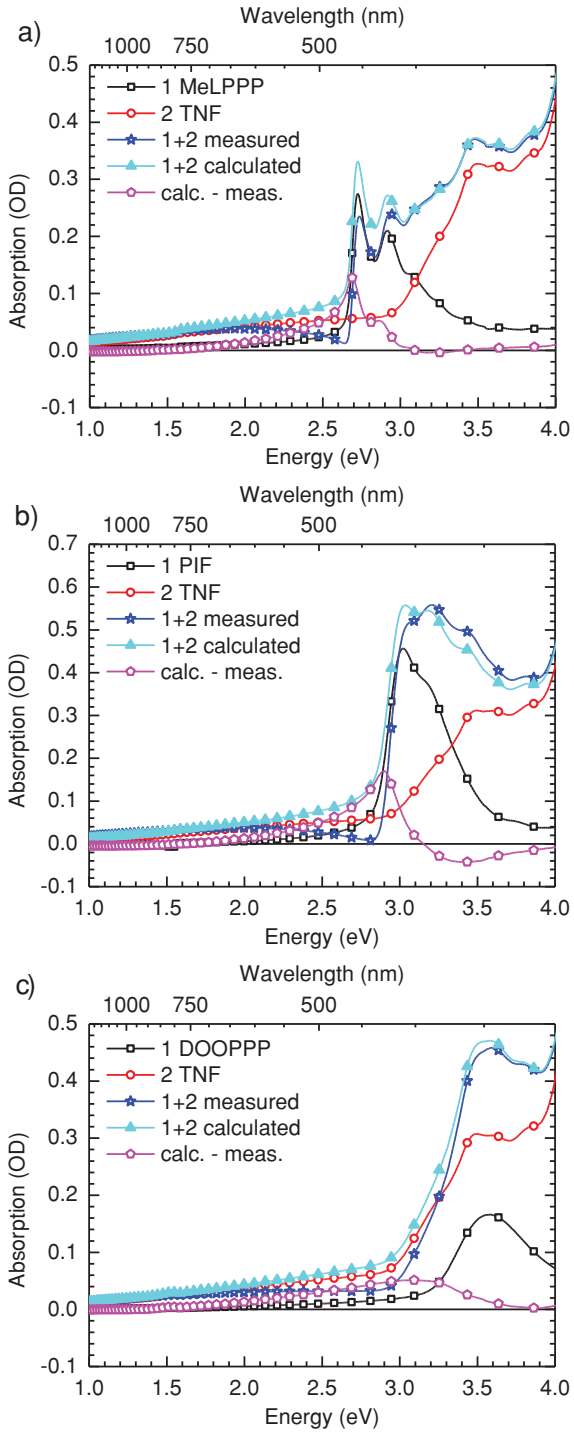

Figure 5. Absorption spectra of a of the different film areas in the samples prepared in configuration I for a) MeLPPP with TNF, b) PIF with TNF, and c) DOOPPP with TNF. Lines and symbols are used analogously to Figure 2. The thickness of the polymer film is about 40 nm that of the TNF layer is about 57 nm.

complete exciton dissociation, which is an order of magnitude lower for MeLPPP than for PIF and DOOPPP, and concomitantly, the amount ground state bleach increases with the effective conjugation length in the PPP-type system.

Table 1. The reduction of the ground state absorption observed for the polymers MEH-PPV, MeLPPP, PIF and DOOPPP in a bilayer with TNF, along with the values of the polymer HOMO energy, the energy difference ΔE_{gap} between the polymer HOMO and the TNF LUMO energy (taken to be –3.9 eV) and the saturation field strength F_{Sat} required for maximum exciton dissociation in a bilayer solar cell structure. F_{Sat}, the MEH-PPV, and TNF energy levels from the literature.[10a,30]

Polymer	Reduction of the ground state absorption	Polymer HOMO [eV]	ΔE_{gap} [eV]	F_{Sat} [10^4 V cm^{-1}]
MEH-PPV	35 %	–5.1	1.2	-
MeLPPP	35%	–5.2	1.3	5
PIF	27%	–5.4	1.5	15
DOOPPP	11%	–5.6	1.6	30

This data suggests that there is a correlation between the amount of ground state absorption that is missing in the bilayer spectra and the efficiency of exciton dissociation. If this is correct one would expect that absorption is in particular missing in the bilayers spectra of well-known efficient solar cell materials. To probe this, we measured the absorption of P3HT and PCPDTBT, two polymers widely used for efficient solar cells, in combination with the acceptor C_{60}. The spectra are shown in the Supporting Information. We find that for the P3HT/C_{60} and the PCPDTBT/C_{60} bilayers, 27% and 32% of the absorption are missing, respectively. The energy gap between the donor HOMO and acceptor LUMO is 0.8 eV and 1.1 eV, respectively, if we take a value of 5.4 eV and 5.1 eV, respectively for the donor HOMO and of 4.3 eV for the C_{60} LUMO. Thus, the results on these solar cell materials in combination with C_{60} are consistent with the findings obtained on the PPV and PPP-type polymers with TNF.

2.4. Quantum Chemical Calculation of the Absorption Spectra

To assist the interpretation of the experimental data, we have calculated the absorption spectra of a model MEH-PV trimer, of TNF and of a sandwich type model dimer where TNF is placed above the MEH-PV trimer using time-dependent density functional theory (TD-DFT). For this, the geometry of the trimer and of TNF were optimized first individually and then the ground state geometry of both molecules together was optimized. Different initial orientations of the two molecules resulted in a very similar, sandwich type final geometry, as detailed in the experimental section. The lowest vertical transition energies with their respective intensities were calculated, and these delta-functions were broadened by multiplying with a Gaussian function to allow comparison with experiment. **Figure 6** shows the absorption spectra obtained for the model MEH-PV trimer, the TNF and the sandwich-type model dimer (dark blue line with stars) with TNF on top of the MEH-PV trimer. For comparison, the sum of the calculated absorption spectra of the TNF and the MEH-PV Trimer is also shown (light blue line with triangles), as well as the difference between the calculated dimer absorption and the sum of the individual absorptions (pink line with circles). The calculations indicate

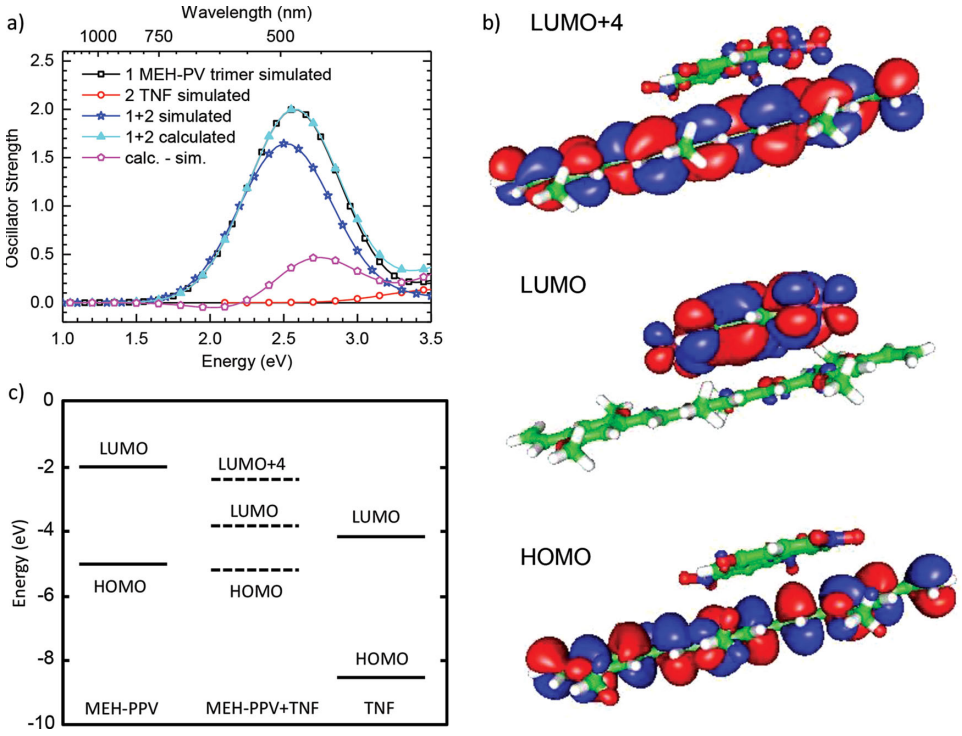

Figure 6. TD-DFT calculations of a model system. a) Calculated absorption spectra of a single MEH-PV trimer, a single TNF and a sandwich-type dimer of MEH-PV trimer with TNF on top of it (dark blue line with stars). For comparison, the sum of the individual spectra of MEH-PV timer and TNF is also shown (light blue line with triangles). The difference between the sum spectrum and the calculated spectrum of the sandwich-type dimer is shown by the pink line with pentagons. b) Orbital plots of the sandwich-type dimer for the HOMO, the LUMO and the LUMO+4. c) Energy level diagram showing the HOMOs and LUMOs of the MEH-PV trimer, the TNF and the sandwich-type dimer formed between them. For the latter, the energy of the LUMO+4 is also indicated.

a reduced absorption of the sandwich-type dimer compared to the MEH-PV trimer as well as a slight additional absorption at the onset of the MEH-PV trimer absorption. In a qualitative manner, this agrees very well with the experimental results displayed in Figure 2. An analysis of the transitions contributing to this absorption band of the donor–acceptor sandwich dimer, centered around 2.5 eV, indicates that it results from a transition from the dimer's HOMO to the dimer's LUMO+4 orbital. Importantly, the dimer's LUMO+4 has some charge density on the TNF molecule, thus suggesting some resonance interaction between the TNF and the PV-trimer to take place. Thus, the lowest optically active excited state, when a TNF acceptor is located on top of a MEH-PV trimer, consists to equal parts of a transition on PV trimer and a transition with some charge-transfer contribution onto the TNF. The excited state analysis also indicates a number of transitions with vanishing oscillator strength roughly around 2 eV.

In Figure 6, we have summarized the HOMO and LUMO energies of the non-interacting MEH-PV trimer and TNF as well as the HOMO, LUMO, and LUMO+4 of the sandwich-type dimer. For reference, the values are also listed in the Supporting Information. In the sandwich-type dimer, the HOMO is stabilized compared to that of the donor MEH-PV, and the LUMO is destabilized compared to the TNF acceptor. The LUMO+4 of the dimer that contributes significantly to the first optically active excited state is between the LUMOs of the MEH-PPV and the TNF.

3. Discussion

To summarize the results obtained on different donor–acceptor systems, we observe a lack in the ground state absorption of donor and acceptor when the two are brought into immediate contact such as to form a bilayer. Through various control measurements, we ascertained that this is a genuine experimental feature. Quantum chemical calculation on the absorption of an adjacent pair of donor and acceptor, that is, a MEH-PV trimer and TNF also yield a reduced intensity of the absorption. As evident from Table 1, the lack of ground state absorption correlates with the energy difference between the donor HOMO and the acceptor LUMO, and with the electrical field strength needed for maximum exciton dissociation. The latter is a measure for the ease of exciton dissociation. Concurrently, lack of ground state absorption also increases with the effective conjugation length in the system of PPP-type polymers.

The energy levels obtained for the donor–acceptor system (Figure 6) are reminiscent of those suggested by Salzmann and co-workers for a ground state (GS) complex. They propose such a species may form when a strong acceptor is brought in contact with a donor with the purpose to p-dope the donor.[8] The GS complex would have a HOMO and LUMO resulting from mixing of the polymer HOMO with the acceptor LUMO, with both electrons for the HOMO of the GS complex being supplied from the former polymer's HOMO. In their picture, the splitting between the frontier orbitals of the GS complex

depends on the intermolecular resonance integral, (β in a Hückel treatment, or referred to as transfer integral t in a tight-binding treatment), and thus on the energy difference between the donor HOMO and the acceptor LUMO. The evidence they provide for this picture is based on photoemission spectroscopy supported by quantum chemical calculations.

We interpret our data in similar fashion. This is, we suggest that upon depositing the acceptor molecule onto the donor polymer, a ground state complex is formed with the frontier orbitals having some hybrid character. The two electrons in the complex HOMO result from the donor polymer, that is, the MEH-PPV. Since the polymer chromophore and the acceptor molecule no longer exist as individual entities after the formation of such a complex, their lowest optical transitions no longer prevail in the same manner. Concurrently, an absorption from the GS complex is expected. In fact, the spectra of Salzmann, Méndez, and co-workers[8a] and in the associated Supporting Information reveal both, a reduction of the S_1 absorption band of the donor as well as the appearance of low energy absorption features. The latter are attributed to transitions of the GS complex. The intensity of the spectral features are not analysed further in their work. Obviously, for the purpose of making solar cells, molecules with weaker acceptor strength are typically chosen than for the purpose of obtaining p-type doping that was the aim in Salzmann's work. For doping, an ideal acceptor will have a LUMO with the same or even with lower energy than the donor's HOMO. For isoenergetic levels, resonance splitting and hybridization of orbitals is at maximum. The finite energy difference ΔE_{gap} between donor HOMO and acceptor LUMO that prevails in a typical donor–acceptor system employed for solar cells, however, implies a weaker mixing. Let us, in a gedanken-experiment, tune ΔE_{gap} from zero offset to a very large limit, in a simple Hückel-type picture. With increasing value of ΔE_{gap}, the splitting reduces, and the hybrid orbitals of the complex acquire a weighted character, with the donor HOMO contributing dominantly to the complex HOMO and the acceptor LUMO prevailing in the complex LUMO. Eventually, for very large ΔE_{gap}, the individual donor HOMO and acceptor LUMO would be retained (**Figure 7**). Let us now consider the expected oscillator strengths. For zero ΔE_{gap} (Figure 7a), the transitions from the complex HOMO to the complex LUMO should have reasonable oscillator strength, since the well mixed character of these orbitals should ensure good overlap of initial and final state wavefunctions, while the absorption from the parent donor and acceptor molecule will be strongly quenched. This is indeed what is observed elsewhere.[8] With increasing ΔE_{gap} (Figure 7b), the low-energy transitions in the complex however acquire a stronger charge-transfer character and a concomitantly weaker oscillator strength, so that their detection requires sensitive techniques such as photothermal deflection spectroscopy. Concomitantly, the bleaching of the parent donor or acceptor absorption should become less pronounced, until for very large ΔE_{gap}, the independent absorption features are retained.

This picture is supported by the experimental data. From Table 1, the correlation between ΔE_{gap} and the bleaching of the absorption is evident. Within the PPP series, ΔE_{gap} reduces with the S_1 energy of the polymer due to the concomitant destabilization of the polymer HOMO, so that the amount of ground state bleach also concurs with the S_1 energy and, implicitly, the effective conjugation length. The reduced extinction of the donor interacting with the acceptor was also observed in the TD-DFT calculations, reproducing the experimental data qualitatively. Quantitatively, the amount for ground state bleach found in the calculation for the MEH-PV trimer/TNF system, that is, 25%, is low compared to the value of 35% measured experimentally for the bilayer formed with MEH-PPV and TNF. We consider that a number of factors contribute to this difference. Some part of this difference may be due to internal reflection at the bilayer interface. Another part may be due to the fact that the calculations have been carried out for a MEH-PV trimer. In the MEH-PPV polymer, however, the effective conjugation length for the ground state geometry has been found in the range of 6 repeat units for the disordered phase, and about twice as long for the planar phase. This larger effective conjugation length with concomitant lower ΔE_{gap} implies a stronger ground state bleach. Multiple interactions, such as clustering of GS complexes proposed by Parashchuk and co-workers,[11] subsequent planarization of the donor after complex formation, the complex formation of one TNF molecule with two or more MEH-PPV chromophores as proposed by Bruevich et al.,[12] or alternatively, of one donor chromophore with several acceptor molecules,[13] are not taken into account. While more extensive computations would be required for a detailed quantitative analysis, the simple initial model calculations employed here are sufficient to qualitatively account for the key features observed experimentally, that is, the appearance of missing ground state absorption.

The interpretation of the data in the picture of an interfacial ground state complex can also elucidate why the amount of missing ground state absorption concurs with the ease of exciton dissociation, as evident in Table 1. Consider an initial arrangement of chromophores in the order donor, donor, acceptor, acceptor, that results in a three-component system of donor, complex, acceptor. As illustrated in **Figure 8**, light absorption by either donor, acceptor or complex, followed by exothermic electron transfer will eventually result in a configuration with an electron removed from the donor and added to the acceptor, with the two opposite,

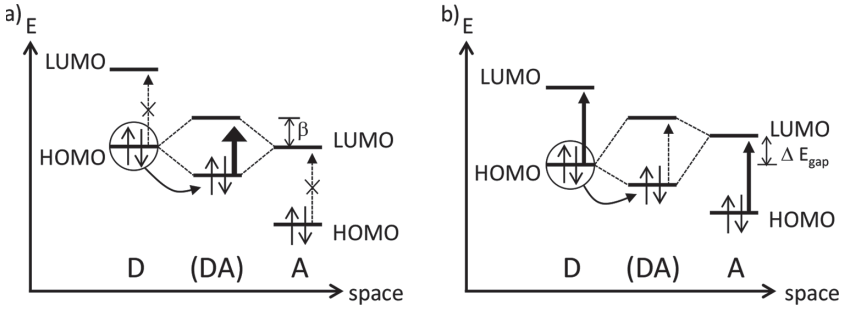

Figure 7. Schematic illustration of the effect of increasing the energy gap ΔE_{gap} between the donor HOMO and acceptor LUMO on the hybridization and thus on the intensity of the transitions for a) zero ΔE_{gap} and for b) increased ΔE_{gap}.

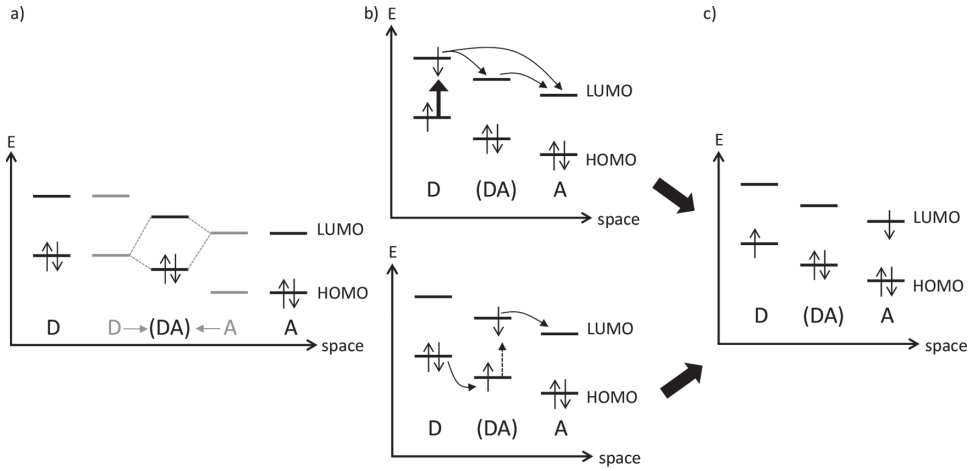

Figure 8. Schematic illustration of the effect of interfacial hybridization on the interfacial energies. a) Formation of a ground state complex at the interface. b) Excitation of the donor or the complex (DA) and subsequent electron transfer. c) the resulting interfacial geminate pair, spatially separated by the complex (DA).

Coulomb-bound charges separated by the complex. The energy levels of the complex form a barrier to geminate recombination in way similar to a small insulating tunnelling barrier[14] or a cascading energy level trilayer system,[15] thus enhancing the probability for the charges to escape their mutual Coulomb potential. The height of the barrier to recombination scales with reducing ΔE_{gap}, and thus with the amount of missing absorption. In earlier work,[10] we have observed that the saturation field strength for complete exciton dissociation, F_{sat}, decreases with increasing conjugation within the PPP series. On the basis of numerical modelling, this was attributed to an increase in kinetic energy of the hole, parameterized through an effective mass, and to the formation of an interfacial electrostatic potential that assists the dissociation process. It is gratifying that the formation of a GS complex proposed here is consistent with the notion of a repulsive interfacial electrostatic potential preventing geminate recombination.

The observation that a ground state complex may form in a donor–acceptor system is well established in the field. For molecular donor–acceptor-type crystals, the electronic interaction between the donor HOMO and the acceptor LUMO has been demonstrated by quantum chemical calculations for crystals with TTF (tetrathiafulvalene) or acene type molecules as donors and TCNQ (tetracyanoquinodimethane) type molecules as acceptor,[16,17] and the importance of the associated absorption of the charge-transfer complex for photocarrier generation has been confirmed.[18–20] For conjugated polymers, the pioneering work of the researchers around Dimitry Paraschuk and Olga Paraschuk on the MEH-PPV/TNF system ascertained the formation of a GS complex by Raman spectroscoy.[12b,21] Using crystallography and modelling, they showed that upon complex formation the MEH-PPV chromophore planarizes and becomes more ordered. GS complexes have further been demonstrated by the observation of weak sub-gap absorption using photothermal deflection spectroscopy (PDS), for example for the PPV-derivative MDMO-PPV, the thiophene-derivative P3HT or the copolymer TFMO (poly[9,9-dioctylfluorene-*co*-*N*-(4-methoxyphenyl)diphenylamine] with the fullerene PCBM.[5a,6,22] While it is well possible to detect the weak low-energy absorption of the GS complexes, PDS is a sophisticated technique that is not routinely available for material screening. Our approach of investigating the existence of a GS complex by focussing on the reduction of the donor and acceptor absorption in a bilayer, in contrast, requires merely a commercial ultraviolet-visible spectrometer, which is a common resource in many laboratories. Due to the observed connection between the amount of ground state bleach and ease of exciton dissociation, this approach may lend itself to screen material combinations for their potential in solar cell applications.

4. Experimental Section

MEH-PPV and C_{60} (99.9% purity) were bought from American Dye Source Inc, polystyrene from Sigma Aldrich. MeLPPP, PIF and DOOPPP were synthesized by the group of U. Scherf as described elsewhere.[23] The precursor PPV was synthesized in Bayreuth using the method described in the literature.[24] The PPV-precursor was converted to PPV by heating for one hour at 165 °C. TNF was also synthesized in Bayreuth following the method of Woofolk and Orchin.[25] The PDI derivative was synthesized by the group of K. Müllen as described as compound PDI-2 in another study.[26]

The samples have been prepared by covering a quadratic fused silica substrate with an about 40 nm polymer donor layer by spin coating from solutions in chlorobenzene at concentrations of 4–10 mg mL^{-1} and at an angular speed of 1000–4000 rpm. The polymer layer is then conscientiously removed from half of the substrate with a cotton bud previously dipped into the solvent. In configuration I, a stripe of acceptor layer is then thermally evaporated through a shadow mask orthogonal onto the polymer layer. In configuration II, the acceptor layer is evaporated in the same geometry yet the substrate is turned over prior to the evaporation, so that polymer and acceptor are separated by the fused silica layer. This results in three different areas: a polymer-only layer, an acceptor-only layer and an area with a superposition of the donor and the acceptor layer. The absorption was recorded using a Cary 5000 (Varian) ultraviolet-visibile (UV–Vis)spectrometer. The film thicknesses were measured by a Dektak profilometer.

For the DFT and TD-DFT calculations, a MEH-PV trimer was used as model system for the MEH-PPV polymer. The geometry of the MEH-PV trimer and the TNF were first optimized separately using the PBE0 hybrid exchange-correlation functional[27] and the turbomole program suite.[28] Then the geometry of both molecules together was optimized

with PBE0 starting from different initial spatial separations and relative orientations of the two molecules. Different relaxations lead to very similar end geometries. As expected for molecules with conjugated π-systems, the configuration in which the two molecular planes are parallel to each other is consistently found as the ground state, lowest energy configuration. The thus obtained gas-phase configuration cannot be expected to be identical to the molecular situation in layered films, but it serves as a reasonable starting point for the exploratory calculations that we aim at in this work.

The ground state configurations of each individual molecule and the combined D–A system served as input to linear-response TD-DFT calculations with the exchange-correlation functional PBE0. The spectra are produced within the range of 0 eV to approximately 4 eV ranging from the lowest to the highest excitation. The lowest 20 excitations were calculated for the donor MEHPPV and the lowest 10 for the acceptor TNF, as these numbers of excited states are sufficient to cover the spectral range of interest. The 30 lowest excitations were determined for the D–A system. These 30 excitations cover the spectral range of interest, that is, up to approximately 3.5 eV. In order to ensure that the optically active excitation in the D–A system is not underestimated due to TD-DFT's well know charge transfer problem[29] we repeated the TD-DFT calculation for the donor–acceptor system with a hybrid functional with an increased amount of exact exchange. This influenced several of the optically dark, low lying excitations noticeably, but changed the energy of the optically active excitation only very little. This finding is in line with the observation that this excitation has only a weak charge-transfer character. Both ground state and excited state calculations used the TZVP basis set. For ease of comparison calculated excitation peaks in the TD-DFT spectra were broadened via a Gaussian function with width chosen such that it roughly matches the experimental width.

Supporting Information

Supporting Information is available from the Wiley Online Library or from the author.

Acknowledgements

The authors acknowledge the Graduate School GRK 1640 of the Deutsche Forschungsgemeinschaft (DFG) for financial support, as well as the Bavarian State Ministry of Science, Research, and the Arts for finanical support through the Collabortive Research Network "Solar Technologies Go Hybrid". The authors thank I. Bauer for the synthesis of TNF and J. Gmeiner for the PPV. Furthermore, the authors thank the group of U. Scherf for synthesizing ladder type polymers and the group of K. Müllen for the PDI derivative. The authors are grateful to C. Grill, E. Riedle, and D. Neher for fruitful discussions and thank B. Tornow for supporting modelling.

Received: January 27, 2014
Revised: June 29, 2014
Published online: August 20, 2014

[1] Heliatek, http://www.heliatek.com/wp-content/uploads/2013/01/130116_PR_Heliatek_achieves_record_cell_effiency_for_OPV.pdf, **2013**.

[2] a) J. L. Bredas, J. E. Norton, J. Cornil, V. Coropceanu, *Acc. Chem. Res.* **2009**, *42*, 1691; b) C. Deibel, V. Dyakonov, *Rep. Prog. Phys.* **2010**, *73*, 096401; c) C. Deibel, T. Strobel, V. Dyakonov, *Adv. Mater.* **2010**, *22*, 4097; d) K. Vandewal, S. Albrecht, E. T. Hoke, K. R. Graham, J. Widmer, J. D. Douglas, M. Schubert, W. R. Mateker, J. T. Bloking, G. F. Burkhard, A. Sellinger, J. M. J. Fréchet, A. Amassian, M. K. Riede, M. D. McGehee, D. Neher, A. Salleo, *Nat. Mater.* **2013**, *13*, 63; e) D. Veldman, O. Ipek, S. C. J. Meskers, J. Sweelssen, M. M. Koetse, S. C. Veenstra, J. M. Kroon, S. S. van Bavel, J. Loos, R. A. J. Janssen, *J. Am. Chem. Soc.* **2008**, *130*, 7721.

[3] a) Y. S. Huang, S. Westenhoff, I. Avilov, P. Sreearunothai, J. M. Hodgkiss, C. Deleener, R. H. Friend, D. Beljonne, *Nat. Mater.* **2008**, *7*, 483; b) A. C. Morteani, P. Sreearunothai, L. M. Herz, R. H. Friend, C. Silva, *Phys. Rev. Lett.* **2004**, *92*, 247402.

[4] a) K. Aryanpour, D. Psiachos, S. Mazumdar, *Phys. Rev. B* **2010**, *81*, 085407; b) C. F. N. Marchiori, M. Koehler, *Synth. Met.* **2010**, *160*, 643.

[5] a) J. J. Benson-Smith, L. Goris, K. Vandewal, K. Haenen, J. V. Manca, D. Vanderzande, D. D. C. Bradley, J. Nelson, *Adv. Funct. Mater.* **2007**, *17*, 451; b) T. Drori, J. Holt, Z. V. Vardeny, *Phys. Rev. B* **2010**, *82*; c) T. Drori, C. X. Sheng, A. Ndobe, S. Singh, J. Holt, Z. V. Vardeny, *Phys. Rev. Lett.* **2008**, 101.

[6] L. Goris, K. Haenen, M. Nesladek, P. Wagner, D. Vanderzande, L. De Schepper, J. D'Haen, L. Lutsen, J. V. Manca, *J. Mater. Sci.* **2005**, *40*, 1413.

[7] P. Pingel, D. Neher, *Phys. Rev. B* **2013**, *87*, 115209.

[8] a) H. Méndez, G. Heimel, A. Opitz, K. Sauer, P. Barkowski, M. Oehzelt, J. Soeda, T. Okamoto, J. Takeya, J. B. Arlin, J. Y. Balandier, Y. Geerts, N. Koch, I. Salzmann, *Angew. Chem. Int. Ed.* **2013**, *52*, 7751; b) I. Salzmann, G. Heimel, S. Duhm, M. Oehzelt, P. Pingel, B. M. George, A. Schnegg, K. Lips, R. P. Blum, A. Vollmer, N. Koch, *Phys. Rev. Lett.* **2012**, *108*, 035502.

[9] a) J. J. M. Halls, K. Pichler, R. H. Friend, S. C. Moratti, A. B. Holmes, *Appl. Phys. Lett.* **1996**, *68*, 3120; b) D. E. Markov, E. Amsterdam, P. W. M. Blom, A. B. Sieval, J. C. Hummelen, *J. Phys. Chem. A* **2005**, *109*, 5266.

[10] a) C. Schwarz, H. Bässler, I. Bauer, J. M. Koenen, E. Preis, U. Scherf, A. Köhler, *Adv. Mater.* **2012**, *24*, 922; b) C. Schwarz, S. Tscheuschner, J. Frisch, S. Winkler, N. Koch, H. Bässler, A. Köhler, *Phys. Rev. B* **2013**, *87*, 155205.

[11] O. D. Parashchuk, V. V. Bruevich, D. Y. Paraschuk, *Phys. Chem. Chem. Phys.* **2010**, *12*, 6021.

[12] a) V. V. Bruevich, T. S. Makhmutov, S. G. Elizarov, E. M. Nechvolodova, D. Y. Paraschuk, *J. Chem. Phys.* **2007**, *127*; b) O. D. Parashchuk, S. Grigorian, E. E. Levin, V. V. Bruevich, K. Bukunov, I. V. Golovnin, T. Dittrich, K. A. Dembo, V. V. Volkov, D. Y. Paraschuk, *J. Phys. Chem. Lett.* **2013**, *4*, 1298.

[13] O. D. Parashchuk, A. Y. Sosorev, V. V. Bruevich, D. Y. Paraschuk, *JETP Lett.* **2010**, *91*, 351.

[14] a) I. H. Campbell, B. K. Crone, *Appl. Phys. Lett.* **2012**, *101*, 023301; b) F. L. Liu, B. K. Crone, P. P. Ruden, D. L. Smith, *J. Appl. Phys.* **2013**, *113*, 044516.

[15] Z. K. Tan, K. Johnson, Y. Vaynzof, A. A. Bakulin, L. L. Chua, P. K. H. Ho, R. H. Friend, *Adv. Mater.* **2013**, *25*, 4131.

[16] L. Zhu, Y. Yi, Y. Li, E.-G. Kim, V. Coropceanu, J.-L. Brédas, *J. Am. Chem. Soc.* **2012**, *134*, 2340.

[17] I. Shokaryev, A. J. C. Buurma, O. D. Jurchescu, M. A. Uijttewaal, G. A. de Wijs, T. T. M. Palstra, R. A. de Groot, *J. Chem. Phys. A* **2008**, *112*, 2497.

[18] K. P. Goetz, D. Vermeulen, M. E. Payne, C. Kloc, L. E. McNeilb, O. D. Jurchescu, *J. Mater. Chem. C* **2014**, *2*, 3065.

[19] J. Tsutsumi, T. Yamada, H. Matsui, S. Haas, T. Hasegawa, *Phys. Rev. Lett.* **2010**, *105*, 226601.

[20] J. Tsutsumi, H. Matsui, T. Yamada, R. Kumai, T. Hasegawa, *J. Phys. Chem. C* **2012**, *116*, 23957.

[21] D. Y. Paraschuk, S. G. Elizarov, A. N. Khodarev, A. N. Shchegolikhin, S. A. Arnautov, E. M. Nechvolodova, *JETP. Lett.* **2005**, *81*, 467.

[22] L. Goris, A. Poruba, L. Hod'akova, M. Vanecek, K. Haenen, M. Nesladek, P. Wagner, D. Vanderzande, L. De Schepper, J. V. Manca, *Appl. Phys. Lett.* **2006**, *88*, 052113.

[23] a) S. P. Huang, G. S. Huang, S. A. Chen, *Synth. Met.* **2007**, *157*, 863; b) U. Scherf, K. Müllen, *Makromol. Rapid Commun.* **1991**, *12*,

489; c) S. Setayesh, D. Marsitzky, K. Müllen, *Macromolecules* **2000**, *33*, 2016.
[24] M. Herold, J. Gmeiner, M. Schwoerer, *Acta. Polym.* **1994**, *45*, 392.
[25] E. O. Woolfolk, M. Orchin, *Org. Synth.* **1948**, *28*, 91.
[26] V. Kamm, G. Battagliarin, I. A. Howard, W. Pisula, A. Mavrinskiy, C. Li, K. Mullen, F. Laquai, *Adv. Energy Mater.* **2011**, *1*, 297.
[27] C. Adamo, V. Barone, *J. Chem. Phys.* **1999**, *110*, 6158.
[28] R. Ahlrichs, M. Bär, M. Häser, H. Horn, C. Kölmel, *Chem. Phys. Lett.* **1989**, *162*, 165.
[29] S. Kümmel, L. Kronik, *Rev. Mod. Phys.* **2008**, *80*, 3.
[30] a) A. L. Holt, J. M. Leger, S. A. Carter, *J. Chem. Phys.* **2005**, *123*, 044704; b) D. P. West, M. D. Rahn, C. Im, H. Bässler, *Chem. Phys. Lett.* **2000**, *326*, 407.